Fashion and Textiles

RESEARCH Open Access

Fabrication of silica/PVA-*co*-PE nanofiber membrane for oil/water separation

Yuanli Chen[1,10†], Hui Fan[2,10†], Xinlin Zha[3,10], Wenwen Wang[4,10], Yi Wu[5], Yi Xiong[6], Kun Yan[7,10], Yuedan Wang[8] and Dong Wang[9*]

*Correspondence: wangdon08@126.com
†Yuanli Chen and Hui Fan contributed equally to this work
[9] Professor, Key Laboratory of Advanced Textile Materials & Application of Hubei Province, Wuhan Textile University, Yangguang Road 1, Wuhan 430073, People's Republic of China
Full list of author information is available at the end of the article

Abstract

High efficiency and anti-pollution oil/water separation membrane has been widely explored and researched. There are a large number of hydroxyl groups on the surface of silica, which has good wettability and can be used for oil-water separation membranes. Hydrophilic silica nanostructures with different morphologies were synthesized by changing templates and contents of trimethylbenzene (TMB). Here, silica nanospheres with radical pores, hollow silica nanospheres and worm-like silica nanotubes were separately sprayed on the PVA-*co*-PE nanofiber membrane (PM). The abundance of hydroxyl groups and porous structures on PM surfaces enabled the absorption of silica nanospheres through hydrogen bonds. Compared with different silica nanostructures, it was found that the silica/PM exhibited excellent super-hydrophilicity in air and underwater "oil-hating" properties. The PM was mass-produced in our lab through melt-extrusion-phase-separation technique. Therefore, the obtained membranes not only have excellent underwater superoleophobicity but also have a low-cost production. The prepared silica/PM composites were used to separate n-hexane/water, silicone oil/water and peanut oil water mixtures via filtration. As a result, they all exhibited efficient separation of oil/water mixture through gravity-driven filtration.

Keywords: PVA-*co*-PE, Radical pore, Hollow structure, Silica, Oil/water separation

Introduction

In recent years, oil spill accidents and oily waste water discharged from industrial processing have caused irreparable ecological damage and huge economic loss (Chen et al. 2015; Liu et al. 2016; Li et al. 2018a, b, c, d, e; Yasukawa et al. 2020). Plankton, algae, worms, crabs and so on have all died, and fish and birds that feed on these creatures have been severely affected. How to efficiently treat water environment problems caused by oil pollution has been a worldwide problem. Therefore, it is urgent to purify water resources to protect human health and keep ecological balance.

To solve the oil pollution problem, many oil/water membranes were utilized. Silica is regarded as functional materials which can be prepared by sol–gel method. There is a large number of Si–OH on the silica surface, making it an excellent choice for the preparation of superhydrophobic membrane (Vitantonio et al. 2018). At present, the preparation of pure silica hydrophilic layer is mainly through the dip-coating method (Chen

et al. 2014; Zhi et al. 2019; Li et al. 2018a, b, c, d, e), in situ polymerization (Yang et al. 2014; Li et al. 2018a, b, c, d, e) and electrostatic attraction (Zhu et al. 2019; Wang et al. 2019). There are two main problems in oil/water separation membrane: surface adsorbed oil pollutants and concentration polarization. Although nanocrystalline silicon has good hydrophilicity, it is easy to cause polarization of water flux and separation efficiency in the preparation of superhydrophilic layer. Surface chemical and physical modification of nano-silica hydrophilic layer is an effective method to improve the oil/water separation capability, such as particle cladding (Li et al. 2018a, b, c, d, e), particle cladding in polymerization (Su et al. 2017), graft (Liao et al. 2019), etc. Nano-silicon with different morphologies and sizes can improve the roughness of the formed super-hydrophilic layer and effectively improve its hydrophilic ability (Li et al. 2018a, b, c, d, e; Kaleekkala et al. 2018). High surface energy and multi-scale roughness can be achieved by forming a homogeneous superhydrophilic modified nano-silicon surface on the membrane fiber (Qing et al. 2020; Liu et al. 2020). The preparation of functionalized silica nanoparticles with 3-amino-propyltriethoxylsilane as a silicon source can greatly improve the properties of the membrane (Khan et al. 2017). It can be seen that silica nanoparticles are used to efficiently separate one of the first materials of the membrane.

Up to date, hollow nanostructure silica/PM has not been used for oil/water separation. For this study, silica nanostructures were obtained by using the hexadecyl trimethyl ammonium bromide (CTAB) or chiral amphiphilic small molecules (L-16Ala5PyPF_6). Hollow silica nanosphere, silica nanosphere with radical pore and worm-like silica nanotube were obtained by tuning the concentration of trimethylbenzene (TMB) and templates. PM is produced in large quantities in our own factory and regarded as a low cost and non-toxic nanofiber membrane. We designed nanofiber separation membranes basing on silica nanostructures spraying on the PMs. Through a variety of wettability measurements, it is found that the hollow SiO_2/PM exhibit super-hydrophilicity and underwater oleophobicity properties. Although various membranes combined silica have been prepared, the preparation of low-cost membrane is an urgent problem. In this work, we have focused our efforts on preparing six kinds of silica/PMs, which have a low-cost and exhibit excellent oil/water separation.

Method

Materials

1-[[4-[(dimethylpheny)azo]dimethylphenyl]azo]-2-Naphthalenol was purchased from Macklin Chemical Company Inc. Erioglaucine disodium salt was purchased from Aladdin Chemistry Co. Ltd. Cellulose acetate butyrate (CAB) was purchased from Eastman Chemical Company. The PP nonwoven substrate was purchased from Kunshan Baoli Nonwoven Co., Ltd. TMB and poly(vinyl alcohol-*co*-ethylene) copolymer were purchased from Sigma-Aldrich (Shanghai) Trading Co. All other agents were obtained from Sinopharm Chemical Reagent Co., Ltd. Except specification, all the above reagents are of analytical grade without further purification.

Characterization

The molecular structure of the L-16Ala5PyPF_6 is shown in Scheme 1, which was synthesized according to the literature (Yang et al. 2006). The NMR characterization of

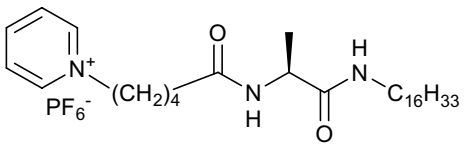

Scheme 1. Molecular structure of L-16Ala5PyPF$_6$

L-16Ala5PyPF$_6$ is shown in Additional file 1: Fig. S1. Fourier transform infrared (FTIR-ATR) spectrum was measured by Bruker Vertex70 spectrometer. Microstructures of samples and X-ray (EDX) mapping were observed at JEOL-7800F field emission scanning electron microscopy (FESEM). H1-NMR spectrum was measured by Bruker AVANCE 400 spectrometer. Elemental analyses were analyzed with a Perkin Elmerseries II CHNS/O analyzer 2400 element analyzer. TEM images were obtained using TecnaiG220 instrument. Contact angles were determined using Kruss DSA30S.

Preparation of silica nanostructures

204 mg CTAB was dissolved in the mixture of 90 mL deionized water and 0.7 mL 2 mol/L NaOH solution at 80 °C. Then, 1.0 mL, 3.0 mL and 6.0 mL TMB were separately added into the mixtures under ultrasound to form a homogeneous solution. After 20 min, 1.0 mL TEOS and 0.8 mL ethyl acetate were added into the above solution and remained at 50 °C with a stirring rate of 800 rpm. Two hours later, the solution was filtered and the powder was washed with ethanol and concentrated hydrochloric acid and further calcined at 550 °C for 5 h to remove the template. The obtained SiO_2 nanospheres were designated as C-SiO_2-1, C-SiO_2-2, C-SiO_2-3.

100 mg L-16Ala5PyPF$_6$, 3 mL methol and 100 mL deionized water were mixed together at 80 °C by stirring with a speed of 1000 rpm to form a clear solution. Then, 0.5 mL, 1.5 mL and 3 mL TMB were separately added into the mixtures under ultrasound to form a homogeneous solution. After 5 min later, 350 μL 2 mol/L NaOH was added and remained stirring. Subsequently, 1 mL tetraethyl orthosilicate (TEOS) was added with stirring for 2 h. Lastly, the solution was filtered and the powder was washed with ethanol and concentrated hydrochloric acid and further calcined at 550 °C for 5 h to remove the template. The obtained SiO_2 nanospheres were named as L-SiO_2-1, L-SiO_2-2, L-SiO_2-3.

Preparation of PM

The PVA-*co*-PE nanofibers were synthesized using a previously published method of our own lab (Wang et al. 2015). The typical synthesis was as follows (Fig. 1), the mixtures of PVA-*co*-PE and CAB were first mixed with a mass ratio of 80:20 and melt extruded from the twin screw extruder. The above mixtures were immersed into acetone solution for 24 h to remove CAB. Then the PVA-*co*-PE nanofibers were left and further dispersed in an aqueous solution to form a stable suspension (Fig. 1b) by a high-speed blender (Fig. 1c). Lastly, PVA-*co*-PE nanofiber suspension was uniformly sprayed on PP (Fig. 1a) substrate and naturally dried to form PM (Fig. 1d). Uniform PVA-*co*-PE nanofiber was found in SEM image (Fig. 1e).

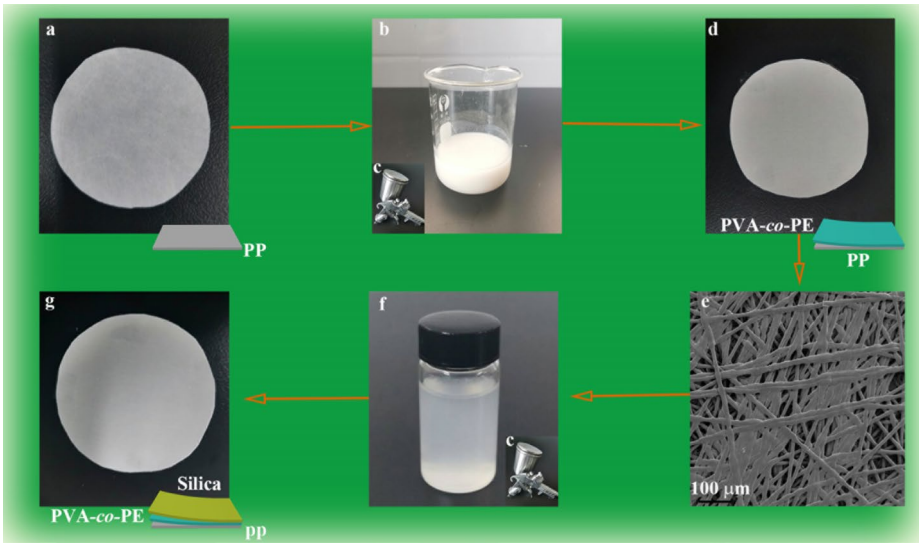

Fig. 1 Preparation process and structures of the PM and silica/PM **a** photograph of PP membrane; **b** PVA-*co*-PE nanofiber suspension; **c** spray gun; **d** photograph of PM; **e** SEM image of the surface of PM; **f** silica suspension and **g** silica/PM

Preparation of silica/PM

In brief, 100 mg SiO_2 samples were dispersed in 15 mL deionized water ultrasounding 2 h to form a uniform suspension solution (Fig. 1f). Lastly, the suspension was sprayed on the surface of the PM and dried it at room temperature. The obtained silica/PMs were designated as C-SiO_2-1/PM, C-SiO_2-2/PM, C-SiO_2-3/PM, L-SiO_2-1/PM, L-SiO_2-2/PM and L-SiO_2-3/PM (Fig. 1g).

Preparation of oil/water separation membrane

The silica/PM membrane is cut into a circular membrane with a radius of 1.35 cm. The volume ratio of oil and water mixture is 1:1. In order to distinguish oil and water clearly, the oil and the water are dyed with 1-[[4-[(dimethylpheny)azo] dimethylphenyl]azo]-2-Naphthalenol (red) and erioglaucine disodium salt (blue), respectively.

Results and discussion

The surface chemical structure of PM

The FTIR-ATR spectra of PM and silica/PMs were shown in Fig. 2. Compared with PM, the characteristic peaks of SiO_2 are all observed in silica/PMs, including 457 cm^{-1} Si–O–Si bending vibration, 810 cm^{-1} Si–O–Si symmetric stretching, 1075 cm^{-1} Si–O asymmetric vibration and 1635 cm^{-1} H–O–H bending vibration. These peaks indicated silica was fabricated on PM successfully.

Morphologies of silica and silica/PM

As shown in Fig. 3a–c, silica nanospheres C-SiO_2-1, C-SiO_2-2, C-SiO_2-3 were obtained using CTAB and TMB as templates. The size of the nanospheres increased by increasing the content of TMB. The diameters of the nanospheres are in the range of 30–80 nm, 60–100 nm, 0.5–1.5 μm, respectively. When 1 mL TMB was added, many pinholes are

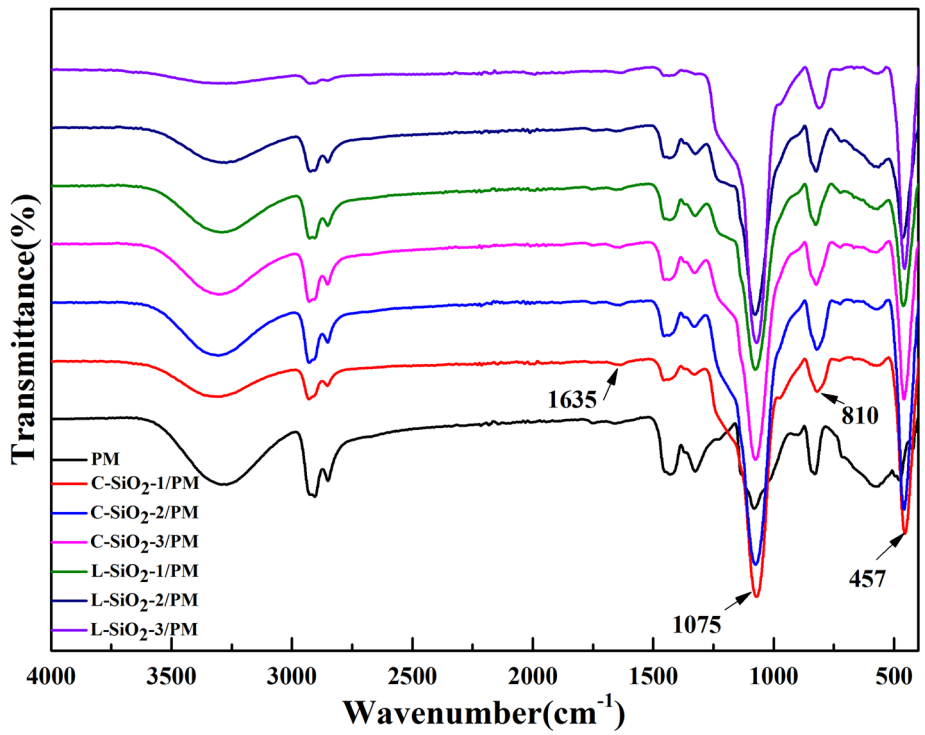

Fig. 2 The FTIR-ATR spectra of PM and silica/PMs

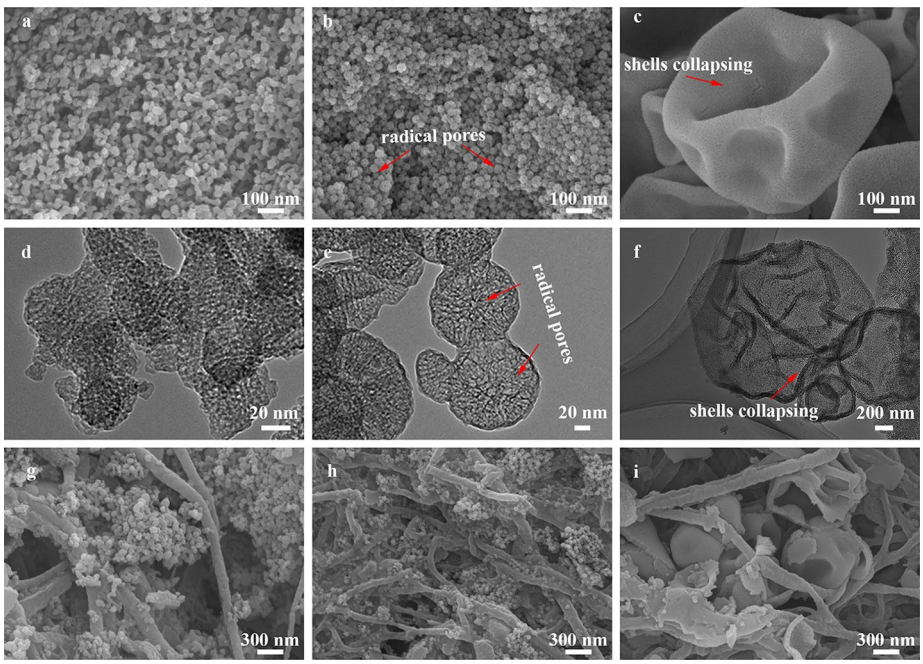

Fig. 3 SEM and TEM images of silica **a**, **d** C-SiO_2-1; **b**, **e** C-SiO_2-2; **c**, **f** C-SiO_2-3. SEM images of silica/PM, **g** C-SiO_2-1/PM; **h** C-SiO_2-2/PM; **i** C-SiO_2-3/PM

found on the surface of silica sample C-SiO_2-1 (Fig. 3d), the pore size are about 1 nm. When TMB were increased into 3 mL, both the hollow nanostructures and radical pores are observed on the surface of the sample C-SiO_2-2 (Fig. 3e). The pore size is about 3.5 nm. The diameter of silica sphere increased dramatically after adding 6 mL TMB and the walls of the shells collapsed. The hollow nanostructures and pinholes are also observed on the surface of the sample C-SiO_2-3 (Fig. 3f). The diameter, pore size and thickness of C-SiO_2-3 are about 0.5–1.5 μm, 6 nm and 25 nm, respectively. In the reaction system of CTAB/TMB, the amount of TMB plays an important role in the forming various nanospheres. When a small amount of TMB is added, it dispersed in the hydrophobic micelle center of CTAB, and further swelled the size of the micelle. Therefore, as the content of TMB increases, the diameter of the obtained silica spheres increases gradually. While the content of TMB is large enough, the TMB oil droplet is used as template, CTAB is adsorbed on the surface of the droplets and further adsorbed TEOS through electrostatic interaction. After the template is removed, a larger hollow silica sphere is obtained (Peng et al. 2014). It was found that silica nanospheres were uniformly embedded into the pores of PM (Fig. 3g–i). SEM images of C-SiO_2-1/PM, C-SiO_2-2/PM and C-SiO_2-3/PM are shown in Fig. 4a, d and g, respectively. EDS mapping images of C-SiO_2-1/PM; C-SiO_2-2/PM; C-SiO_2-3/PM are shown in Fig. 4b, c, e, f and g–i, respectively. Red dots represent element of silicon. EDS mapping images of the silica/PMs were also confirmed that the silicons (red dots) were uniformly dispersed on the surfaces of PMs (Fig. 4).

As shown in Fig. 5, worm-like silica nanotubes and nanospheres L-SiO_2-1, L-SiO_2-2, L-SiO_2-3 were obtained using L-16AlaPyPF_6 and different count of TMB as templates.

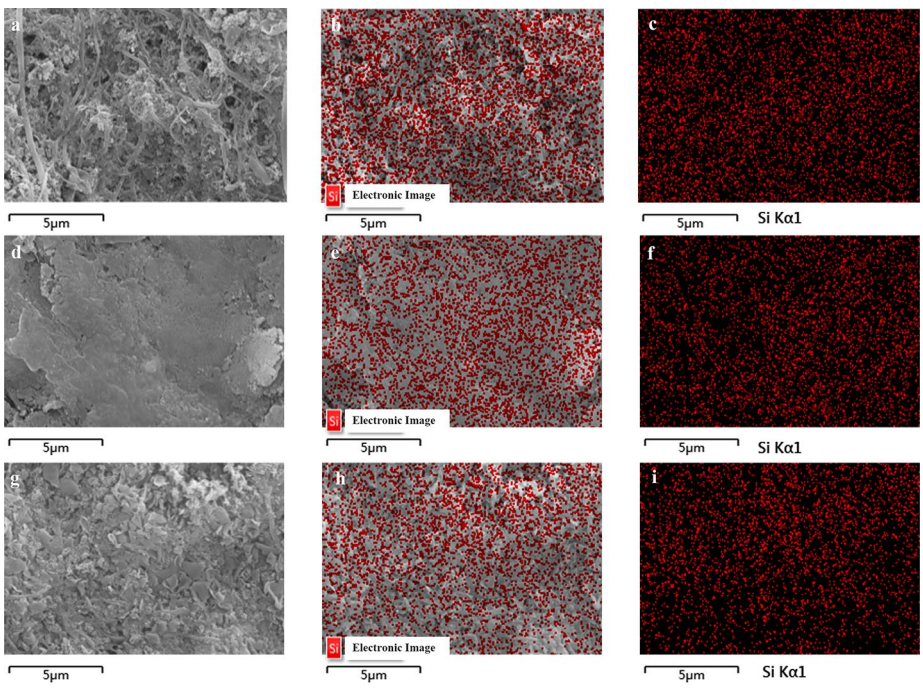

Fig. 4 SEM images of C-SiO_2-1/PM (**a**), C-SiO_2-2/PM (**d**) and C-SiO_2-3/PM (**g**). EDS mapping images of C-SiO_2-1/PM (**b**, **c**), C-SiO_2-2/PM (**e**, **f**) and C-SiO_2-3/PM (**h**, **i**). Red dots represent element of silicon

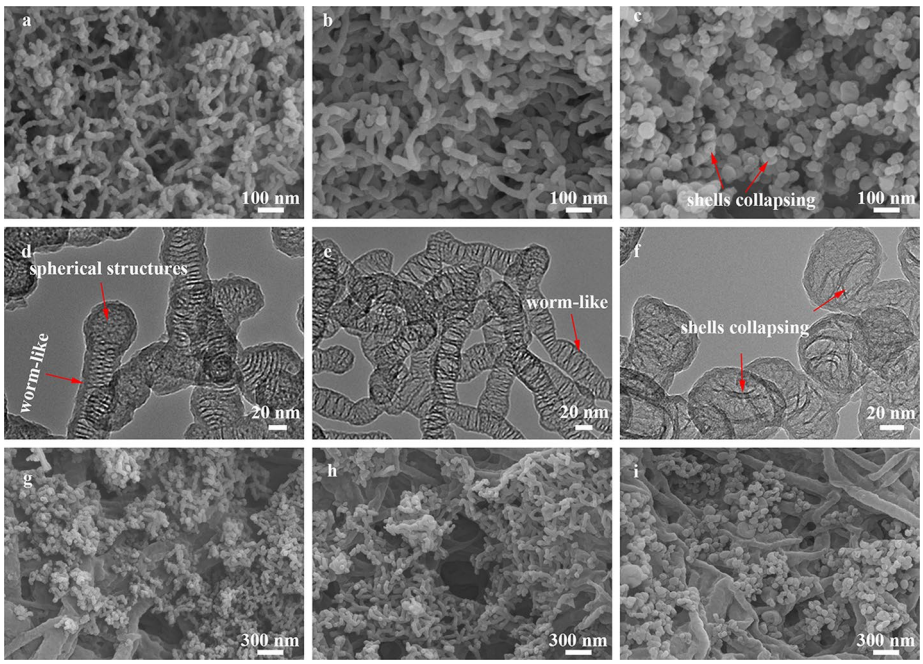

Fig. 5 SEM and TEM images of silica **a**, **d** L-SiO_2-1; **b**, **e** L-SiO_2-2; **c**, **f** L-SiO_2-3. SEM images of silica/PM **g** L-SiO_2-1/PM; **h** L-SiO_2-2/PM; **i** L-SiO_2-3/PM

For L-SiO_2-1, worm-like silica nanorods with two ends of spherical structures were obtained after adding 0.5 mL TMB (Fig. 5a). TEM image confirmed they were hollow nanotubes (Fig. 5d). The length and diameter of the nanotubes are about 130–350 nm and 30–45 nm. When TMB was increased to 1.5 mL, uniform silica nanotubes L-SiO_2-2 with worm-like structures were found in Fig. 5b, e. The length and diameter of L-SiO_2-2 are about 100–325 nm and 47–63 nm, respectively. However, for sample L-SiO_2-3, only silica nanospheres were identified in Fig. 5c after adding 3.0 mL TMB. As shown in Fig. 5f, the spheres are hollow structures with shells collapsing. The diameter is about 58–600 nm and many mesopores are found on the surface of the nanospheres. Chiral small molecules assembled a bundle-like structure through hydrogen bonds. When the content of TMB is low, the self-assembly of chiral small molecules is used as a template. Worm-like structure is obtained by removing the template. With the content of TMB increasing, TMB oil droplets serve as template. L-16Ala5PyPF_6 is adsorbed on the surface of the oil droplets, and silica is adsorbed on L-16Ala5PyPF_6 by electrostatic action. The hollow silica sphere can be obtained by removing the template. As shown in Fig. 5g–i, worm-like silica nanotubes and nanospheres were uniformly fabricated on PM. Due to the large number of hydroxyl groups on the surface of these silicas, they have very good hydrophilicity. Therefore, spraying these silicon on the PM film can significantly improve the hydrophilicity of PM. SEM images of L-SiO_2-1/PM, L-SiO_2-2/PM and L-SiO_2-3/PM are shown in Fig. 6a, d and g, respectively. EDS mapping images of L-SiO_2-1/PM; L-SiO_2-2/PM; L-SiO_2-3/PM are shown in Fig. 6b, c, e, f and g–i, respectively. Blue dots represent element of silicon. As is shown in Fig. 6, the silicas prepared by L-16Ala5PyPF_6/TMB are uniformly distribute on the surface of the films.

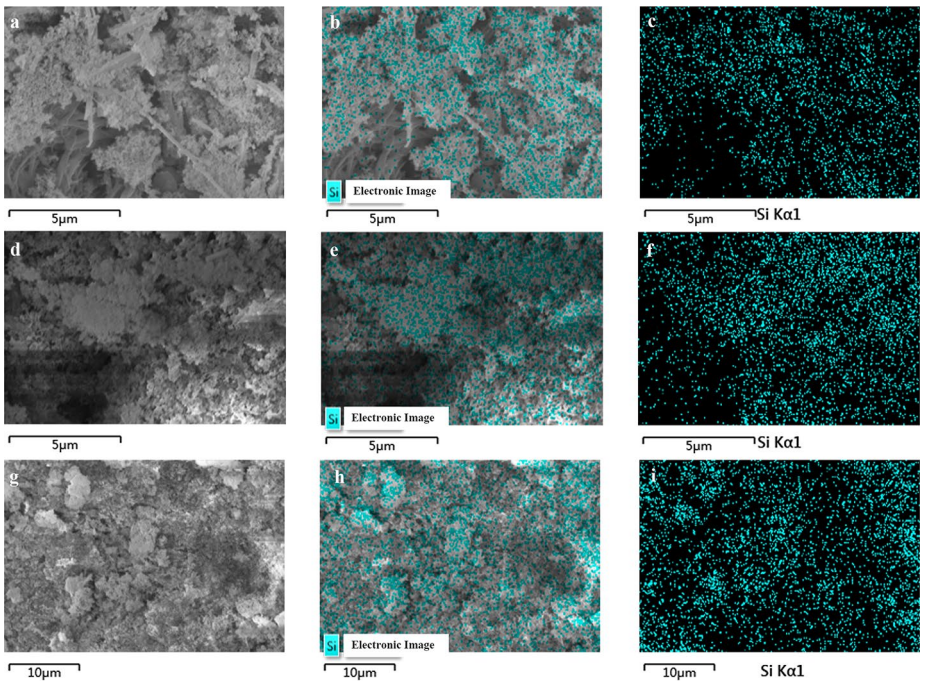

Fig. 6 SEM images of L-SiO_2-1/PM (**a**), L-SiO_2-2/PM (**d**) and L-SiO_2-3/PM (**g**). EDS mapping images of L-SiO_2-1/PM (**b**, **c**); L-SiO_2-2/PM (**e**, **f**); L-SiO_2-3/PM (**h**, **i**). Blue dots represent element of silicon

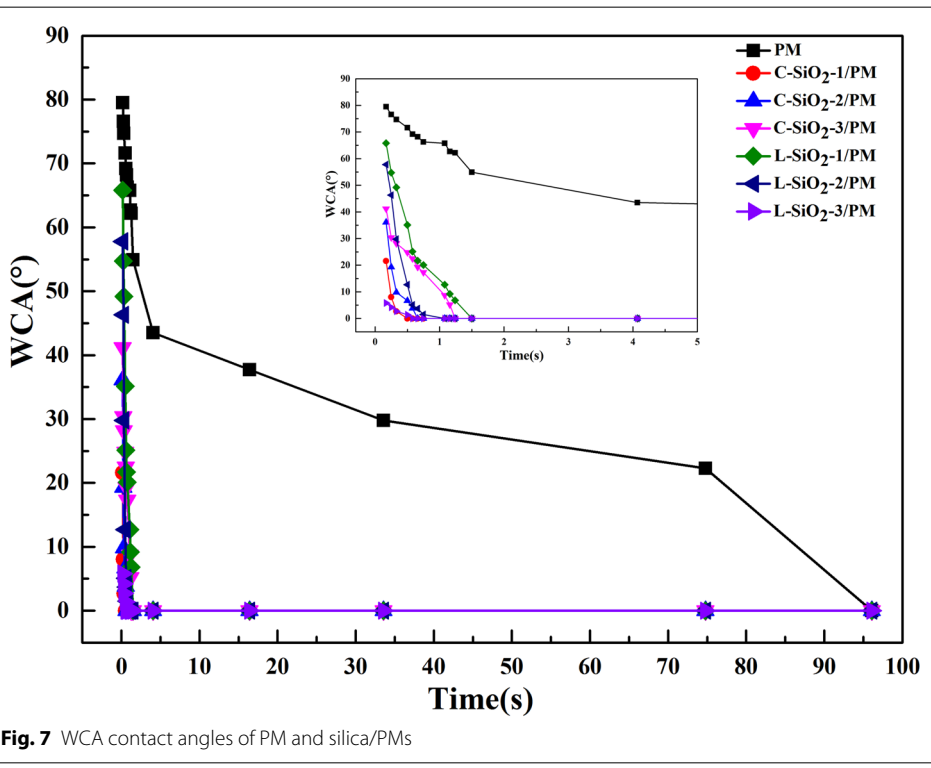

Fig. 7 WCA contact angles of PM and silica/PMs

Changes of WCA contact angles over time

The hydrophilicity of the different membranes' surfaces were monitored by water contact angle (WCA) tests which are shown in Fig. 7. It took about 96 s when the contact angle of the PM from 79.5° to 0°. The embedded image in Fig. 7 is an enlarged view of the contact angle of silica/PMs within 5 s, from which we can see that the slowest silica/PM took about 1.5 s when the contact angle became 0°, while the fastest film took only 0.5 s. It can be concluded that the hydrophilicity was improved after PM embedded silica nanospheres with radical pores, hollow silica nanospheres and worm-like silica nanotubes. Since there are a large number of hydroxyl groups on the surface of silica, and there are a large number of pores inside these silica balls or silica tubes, the hydrophilic properties of the membrane can be greatly improved. It provides the possibility for the separation of oil and water membrane. EDS mapping images of the silica/PM were also confirmed that the silicas were uniformly dispersed on the surface of PMs (Figs. 4 and 6).

Oil/water separation

As shown in Fig. 8a, we put the prepared C-SiO_2-2/PM into a beaker filled with water, and then dropped the chloroform dyed with 1-[[4-[(dimethylpheny)azo]dimethylphenyl]azo]-2-Naphthalenol on the surface. Because chloroform is denser than water, when pink chloroform oil drops onto the surface of the underwater film, which showed hydrophobic characteristics on the surface of the membrane. When we took n-hexane oil droplet dyed with 1-[[4-[(dimethylpheny)azo]dimethylphenyl]azo]-2-Naphthalenol, which is less dense than water, it's found that the pink n-hexane oil drops below the membrane also exhibited hydrophobic properties. It is worth noting that when we suck the chloroform away from the membrane with a straw (Fig. 8c, d), no oil droplets are left on the membrane (Fig. 8e), so the membrane can be used as an oil repellent. Due to the super-hydrophilicity in air and super hydrophobic oil underwater (Fig. 8a, b), C-SiO_2-2/PM can be used in oil—water separation. The separation property of the C-SiO_2-2/PM is further studied for n-hexane/water mixtures. N-hexane and water (dyed by erioglaucine disodium salt) (1:1 v/v) are put it in the oil

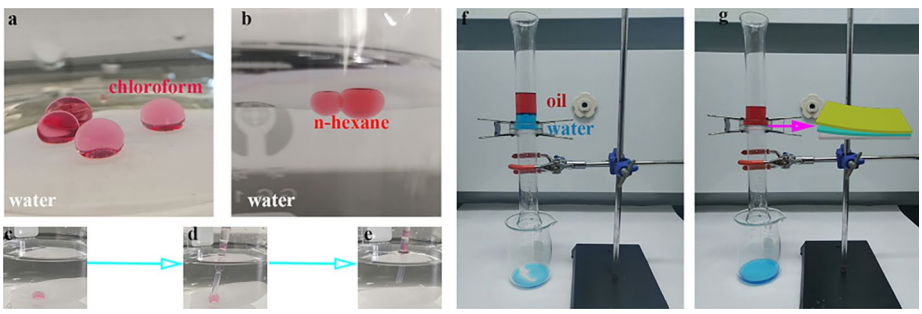

Fig. 8 Photographs of oil droplets underwater. Chloroform, n-hexane (red); water (blue). **a** Chloroform (bottom side, heavier than water), **b** n-hexane (top side, lighter than water) in water on the surface of silica/PM. **c**–**e** The images of chloroform oil droplet nonadhesive on the surface of the silica/PM. **f**, **g** The photographs of the measurement of the oil/water separation performance of silica/PM, **f** before separation and **g** after separation, respectively

and water separator. Since the density of n-hexane is lighter than water, n-hexane is distributed above the water. As a result, the water penetrated through the SiO_2/PM while the oil is intercepted (Fig. 8f, g). Therefore, silica/PM can effectively separate oil and water mixture through gravity-driven filtration. Therefore, we carried out the study of oil–water separation with six kinds of films prepared above. It's found that the membranes can also effectively separate n-hexane/water, silicone oil/water and peanut oil/water mixtures. The separation efficiencies are listed in Fig. 9. The results show that all the silica/PMs exhibit high separation efficiency (> 98%) for oil/water mixtures.

Conclusions

The PM was firstly combined with hollow silica nanosphere, silica nanosphere with radical pore and worm-like silica nanotube in oil–water separation. The surface chemical structures of silica/PMs were characterized by SEM, EDS mapping, TEM and IR-ATR spectra. The contact angle tests demonstrated that super-hydrophilicity in air and underwater "oil-hating" properties. Therefore, the silica/PMs can effectively three different oil. Furthermore, the oil drops are nonadhesive on the surface of the

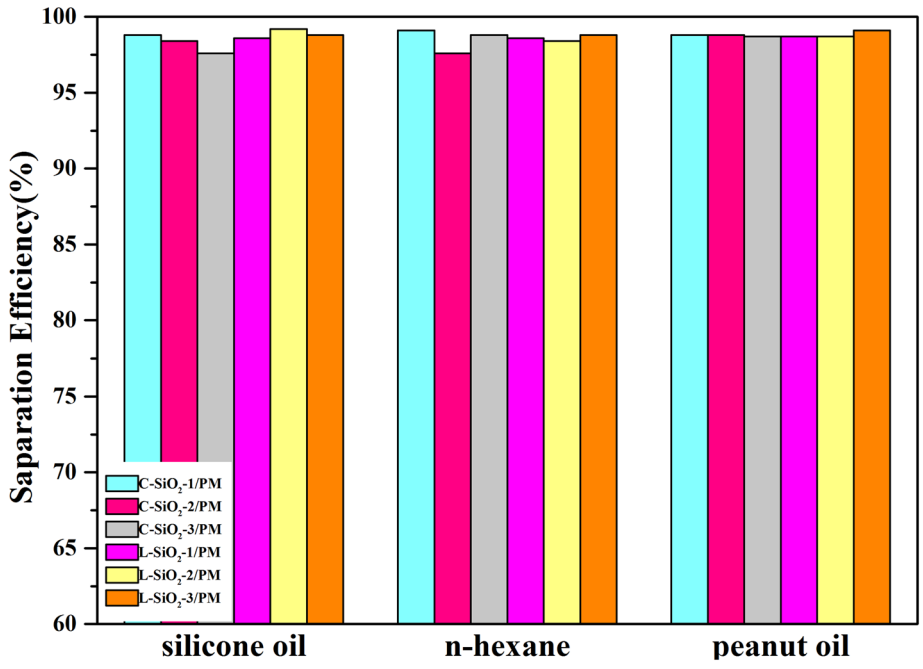

Fig. 9 Oil/water separation efficiencies of different silica/PMs

silica/PM. In the future research, silica nanostructures with more morphologies will be carried out in oil–water separation applications.

Supplementary Information

The online version contains supplementary material available at https://doi.org/10.1186/s40691-021-00252-x.

Additional file 1: Fig. S1. H1-NMR of L-16Ala5PyPF$_6$ in DMSO.

Acknowledgements
The authors are grateful for the financial support of the National Natural Science Foundation of China [Grant number 51603155, 2017] and Hubei Province Education Department Project [Grant number Q20191708, 2019].

Authors' contributions
YC and HF: conception of the study, writing—review and editing; XY, KY and YW: investigation; WW and YW: data curation; DW: supervision. All authors read and approved the final manuscript.

Funding
National Natural Science Foundation of China [Grant number 51603155, 2017] and Hubei Province Education Department Project [Grant number Q20191708, 2019].

Availability of data and materials
The datasets used and/or analysed during the current study are available from the corresponding author on reasonable request.

Ethics approval and consent to participate
Not applicable.

Consent for publication
Not applicable.

Competing interests
The authors declare that they have no competing interests.

Author details
[1] Phd, School of Materials Science and Engineering, Wuhan Textile University, Yangguang Road 1, Wuhan 430073, People's Republic of China. [2] Graduate student, School of Materials Science and Engineering, Wuhan Textile University, Yangguang Road 1, Wuhan 430073, People's Republic of China. [3] Graduate student, School of Materials Science and Engineering, Wuhan Textile University, Yangguang Road 1, Wuhan 430073, People's Republic of China. [4] Associate professor, School of Materials Science and Engineering, Wuhan Textile University, Yangguang Road 1, Wuhan 430073, People's Republic of China. [5] Phd, Key Laboratory of Advanced Textile Materials & Application of Hubei Province, Wuhan Textile University, Yangguang Road 1, Wuhan 430073, People's Republic of China. [6] Phd, Key Laboratory of Advanced Textile Materials & Application of Hubei Province, Wuhan Textile University, Yangguang Road 1, Wuhan 430073, People's Republic of China. [7] Phd, School of Materials Science and Engineering, Wuhan Textile University, Yangguang Road 1, Wuhan 430073, People's Republic of China. [8] Associate professor, School of Materials Science and Engineering, Wuhan Textile University, Yangguang Road 1, Wuhan 430073, People's Republic of China. [9] Professor, Key Laboratory of Advanced Textile Materials & Application of Hubei Province, Wuhan Textile University, Yangguang Road 1, Wuhan 430073, People's Republic of China. [10] Key Laboratory of Advanced Textile Materials & Application of Hubei Province, Wuhan Textile University, Yangguang Road 1, Wuhan 430073, People's Republic of China.

Received: 31 August 2020 Accepted: 6 February 2021
Published online: 05 April 2021

References

Chen, K. L., Zhou, S. X., & Wu, L. M. (2015). Self-healing underwater superoleophobic and antibiofouling coatings based on the assembly of hierarchical microgel spheres. *ACS Nano, 10*(1), 1386–1394. https://doi.org/10.1021/acsnano.5b06816.

Chen, Y. N., Xue, Z. X., Liu, N., et al. (2014). Fabrication of a silica gel coated quartz fiber mesh for oil–water separation under strong acidic and concentrated salt conditions†. *RSC Advances, 4,* 11447–11450. https://doi.org/10.1039/C3RA46661B.

Kaleekkala, N. J., Radhakrishnanb, R., Sunil, V., et al. (2018). Performance evaluation of novel nanostructured modified mesoporous silica/polyetherimide composite membranes for the treatment of oil/water. *Separation and Purification Technology Emulsion, 205,* 32–47. https://doi.org/10.1016/j.seppur.2018.05.007.

Khan, S. A., Zulfiqar, U., et al. (2017). Fabrication of superhydrophobic filter paper and foam for oil–water separation based on silica nanoparticles from sodium silicate. *Journal of Sol-Gel Science and Technology, 81,* 912–920. https://doi.org/10.1007/s10971-016-4250-6.

Li, H. Q., Li, T., Li, X. J., et al. (2018c). Vapor-liquid interfacial reaction to fabricate superhydrophilic and underwater superoleophobic thiol-ene/silica hybrid decorated fabric For oil/water separation. *Applied Surface Science, 427,* 92–101. https://doi.org/10.1016/j.apsusc.2017.08.022.

Li, M. F., Li, Y. Q., Chang, K. Q., et al. (2018b). The poly(vinyl alcohol-co-ethylene) nanofiber/silica coated composite membranes for oil/water and oil-in-water emulsion separation. *Composites Communications, 7,* 69–73. https://doi.org/10.1016/j.coco.2018.01.001.

Li, M., Li, Y., Xue, F., & Jing, X. L. (2018e). Water-based acrylate copolymer/silica hybrids for facile preparation of robust and durable superhydrophobic coatings. *Applied Surface Science, 447,* 489–499. https://doi.org/10.1016/j.apsusc.2018.04.008.

Li, Y., Shang, X. Z., & Zhang, B. Q. (2018d). One-step fabrication of the pure-silica zeolite beta coating on steel mesh for efficient oil/water separation. *Industrial & Engineering Chemistry Research, 57*(51), 17409–17416. https://doi.org/10.1021/acs.iecr.8b04172.

Li, Y. T., Wang, Y. F., Gao, Y. Z., et al. (2018a). Seawater toilet flushing sewage treatment and nutrients recovery by marine bacterial-algal mutualistic system. *Chemosphere, 195,* 70–79. https://doi.org/10.1016/j.chemosphere.2017.12.076.

Liao, Z. W., Wu, G. X., Lee, D. Y., & Yang, S. (2019). Ultrastable underwater anti-oil fouling coatings from spray assemblies of polyelectrolyte grafted silica nanochains. *Applied Surface Science, 11*(14), 13642–13651. https://doi.org/10.1021/acsami.8b19310.

Liu, J., Wang, L., Guo, F., Hou, L., et al. (2016). Opposite and complementary: a superhydrophobic-superhydrophilic integrated system for high-flux, high-efficiency and continuous oil/water separation. *Journal of Materials Chemistry A, 4,* 4365–4370. https://doi.org/10.1039/C5TA10472F.

Liu, W. D., Xiang, S. Y., Liu, X. Y., & Yang, B. (2020). Underwater superoleophobic surface based silica hierarchical cylinder arrays with a low aspect ratio. *ACS Nano, 14*(7), 9166–9175. https://doi.org/10.1021/acsnano.0c04670.

Peng, J., Liu, J., Liu, J., et al. (2014). Fabrication of core-shell structured mesoporous silica nanospheres with dually oriented mesochannels through pore engineering. *Journal of Materials Chemistry A, 2,* 8118–8125. https://doi.org/10.1039/C4TA00899E.

Qing, W. H., Li, X. H., Wu, Y. F., et al. (2020). In situ silica growth for superhydrophilic-underwater superoleophobic Silica/PVA nanofibrous membrane for gravity-driven oil-in-water emulsion separation. *Journal of Membrane Science, 612,* 118476. https://doi.org/10.1016/j.memsci.2020.118476.

Su, X. J., Li, H. Q., Lai, X. J., et al. (2017). Vapor-liquid sol-gel approach to fabricating highly durable and robust superhydrophobic polydimethylsiloxane/silica surface on polyester textile for oil-water separation. *ACS Applied Materials & Interfaces, 9*(33), 28089–28099. https://doi.org/10.1021/acsami.7b08920.

Vitantonio, G. D., Wang, T. C., Haase, M. F., et al. (2018). Robust Bijels for reactive separation via silica-reinforced nanoparticle layers. *ACS Nano, 13*(1), 26–31. https://doi.org/10.1021/acsnano.8b05718.

Wang, J. T., & Wang, H. F. (2019). Ultra-hydrophobic and mesoporous silica aerogel membranes for efficient separation of surfactant-stabilized water-in-oil emulsion separation. *Separation and Purification Technology, 212,* 597–604. https://doi.org/10.1016/j.seppur.2018.11.078.

Wang, W. W., Zhao, Q. H., Luo, M. Y., et al. (2015). Immobilization of firefly luciferase on PVA-co-PE nanofibers membrane as biosensor for bioluminescent detection of ATP. *ACS Applied Materials & Interfaces, 7*(36), 20046–20052. https://doi.org/10.1021/acsami.5b07339.

Yang, S., Si, Y., Fu, Q. H., et al. (2014). Superwetting hierarchical porous silica nanofibrous membranes for oil/watermicroemulsion separation†. *Nanoscale, 6,* 12445–12449. https://doi.org/10.1039/C4NR04668D.

Yang, Y. G., Suzuki, M., Owa, S., et al. (2006). Control of mesoporous silica nanostructures and pore-architectures using a thickener and a gelator. *Journal of the American Chemical Society, 129*(3), 581–587. https://doi.org/10.1021/ja064240b.

Yasukawa, M., Mehdizadeh, S., Sakurada, T., et al. (2020). Power generation performance of a bench-scale reverse electrodialysis stack using wastewater discharged from sewage treatment and seawater reverse osmosis. *Desalination, 491,* 114449. https://doi.org/10.1016/j.desal.2020.114449.

Zhi, D. F., Wang, H. H., Jiang, D., et al. (2019). Reactive silica nanoparticles turn epoxy coating from hydrophilic to superrobust superhydrophobic. *RSC Advances, 9,* 12547–12544. https://doi.org/10.1039/C8RA10046B.

Zhu, Z. G., Li, Z. Y., Zhong, L. L., et al. (2019). Dual-biomimetic superwetting silica nanofibrous membrane for oily water purification. *Journal of Membrane Science, 572,* 73–81. https://doi.org/10.1016/j.memsci.2018.10.071.

Publisher's Note